Electronic Supplementary Information

The Enhancement of Li-ion Conductivity in 2D Metalloid Organic Frameworks via Nodal Element Substitution

Lisha Liang,[a] Yan Wang,[a] Shumaila Ashraf,[a] and Pengfei Li*[a,b]

a. Frontiers Science Center for High Energy Material, Key Laboratory of Cluster Science, Ministry of Education, Beijing Key Laboratory of Photoelectronic/Electrophotonic Conversion Materials, School of Chemistry and Chemical Engineering, Beijing Institute of Technology, No. 5, Zhongguancun South Street, Haidian District, Beijing 100081, P. R. China. E-mail: lipengfei@bit.edu.cn

b. Advanced Research Institute of Multidisciplinary Science, Beijing Institute of Technology, Zhuhai, No.6, Jinfeng Road, Tangjiawan, Zhuhai, 519088, P. R. China.

1. Experimental section

Materials and instruments

9,10-dimethyl-2,3,6,7-tetrahydroxy-anthracene was supplied with Jilin Chinese Academy of Sciences - Yanshen Technology Co., Ltd. Silicon dioxide (SiO_2) was purchased from Macklin chemical. Germanium oxide (GeO_2) was purchased from Aladdin.

^1H NMR spectra were measured on a Bruker Advance III 400 MHz spectrometer with tetramethylsilane (TMS) as the internal standard. Powder X-ray diffraction (PXRD) was recorded on a Rigaku MiniFlex 600 diffractometer using Cu Kα X-ray source with 40 kV voltage and 50 mA current. Fourier transform infrared (FT-IR) spectra were performed on Bruker ALPHA spectrometer in the range of 400~4000 cm$^-$^{1}. N_2 sorption isotherms were carried out at 77 K on a Quantachrome Instrument Autosorb-iQ after degassed under vacuum at 120 °C for 12 h. The pore size distributions were determined by non-local density function theory (NLDFT). Thermogravimetric analysis (TGA) was conducted on a NETZSCH Proteus STA 449F5 analyzer by heating the sample within the temperature range of 35~800 °C under N_2 atmosphere at a heating rate of 5 °C /min. Scanning electron microscopy (SEM) images were obtained from a JEOL model JSM-7500F scanning electron microscope. Transmission electronic microscopy (TEM) was carried out with a JEOL model JEM-2100 microscope at 200 kV. X-ray photoelectron spectroscopy (XPS) was performed by using Thermo scientific ESCALAB 250Xi with Al Kα radiation. The water contact angle was measured by the sessile drop method using an optical surface analyzer (OSA200, Ningbo NB Scientific Instruments).

Synthesis of SiOF-Li:

9,10-dimethyl-2,3,6,7-tetrahydroxy-anthracene (DMTHA) (100 mg, 0.375 mmol), silica gel (15 mg, 0.25 mmol) and 0.55 mL of 1.0 M alkali methoxide solution in anhydrous methanol (9.5 mL) inside a 25 mL Teflon-lined steel autoclave. The autoclave was sealed and placed in an oven heated at 180 °C for 4 days. The precipitate was washed with anhydrous acetone and evacuated at room temperature for 12 h.

Synthesis of GeOF-Li:

9,10-dimethyl-2,3,6,7-tetrahydroxy-anthracene (DMTHA) (100 mg, 0.375 mmol), germanium oxide (26 mg, 0.25 mmol) and 0.55 mL of 1.0 M alkali methoxide solution in anhydrous methanol (9.5 mL) inside a 25mL Teflon-lined steel autoclave. The autoclave was sealed and placed in an oven heated at 180 °C for 3 days. The precipitate was washed with anhydrous acetone and evacuated under 60 °C for 12 h.

Ion conductivity tests:

Pristine or infiltrated SiOF-Li or GeOF-Li was compressed into pellets under a pressure of 3 MPa for 30 seconds. Inside a glove box, these compressed pellets were securely positioned between two stainless-steel electrodes, arranged in a coin cell configuration. Subsequently, electrochemical impedance spectroscopy EIS measurements were conducted to record the impedance curves across a frequency range spanning from 1 Hz to 10^6 Hz with a signal amplitude of 100 mV. The conductivity (σ) of the materials was then determined using an appropriate formula.

$$\sigma = \frac{l}{R \times A}$$

Where l is the thickness of the pellet in cm, R is the resistance (Ω) obtained by the simulation of equivalent circuit, and A is the sample area (cm^2) in contact with electrode.

Density functional theory (DFT) calculations:

DFT calculations were conducted using a plane wave basis set with the projector augmented wave (PAW) method under the generalized gradient approximation (GGA) in the Vienna ab initio simulation package (VASP).[1,2] A kinetic energy cutoff of 500 eV was applied for all calculations. Brillouin-zone integration was performed using the Monkhorst–Pack scheme, employing a k-point mesh of $(2 \times 2 \times 1)$ for geometry optimization.[3] Structures were optimized by relaxing all atomic positions until the forces fell below 0.01 eV Å^{-1}. Activation energy calculations were carried out using the climbing-image nudged elastic band (CI-NEB) method in supercells consisting of $1 \times 1 \times 2$ unit cells. Seven intermediate images were generated to represent the transition between the initial and final states along the ion diffusion pathway, with lattice parameters kept fixed while the moving ions were allowed to relax during the NEB calculations.
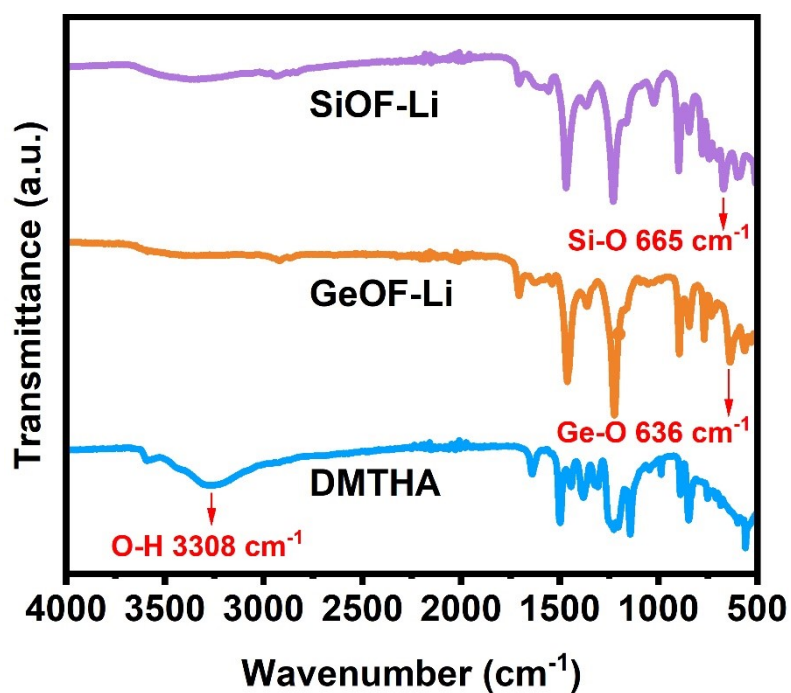
2. Figures and Tables

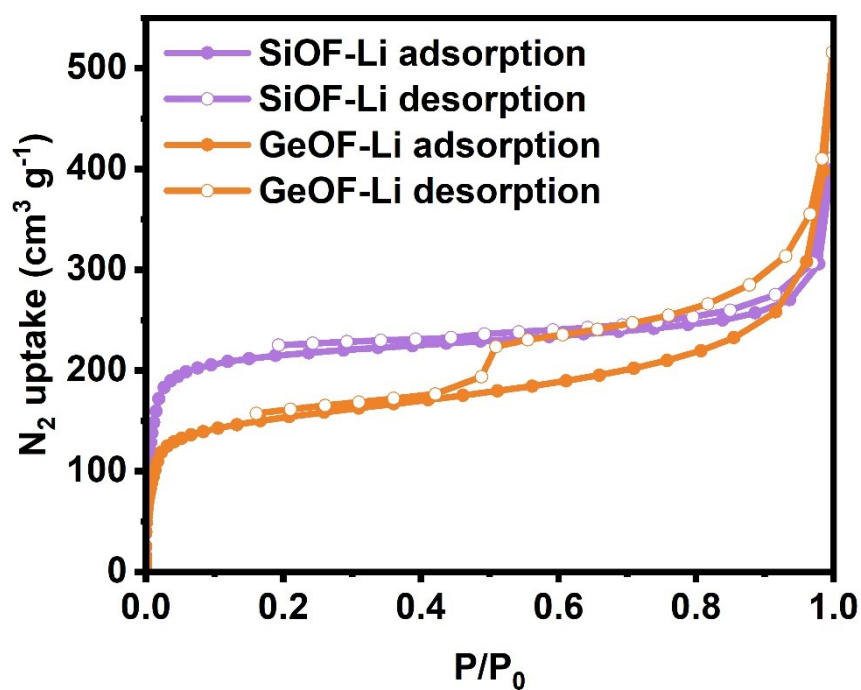**Fig. S1** Fourier-transform infrared spectra of SiOF-Li, GeOF-Li, and DMTHA.

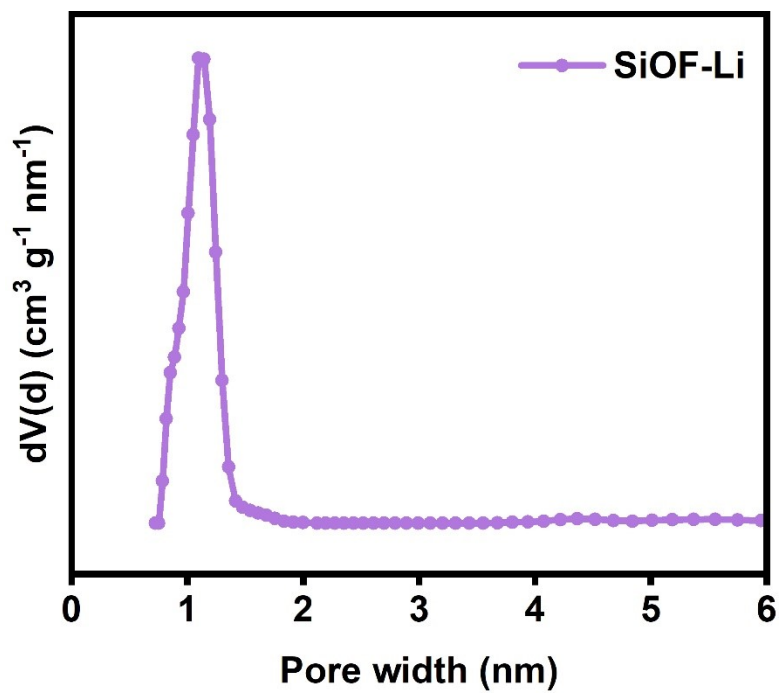**Fig. S2** N_2 isotherms of SiOF-Li and GeOF-Li at 77 K.

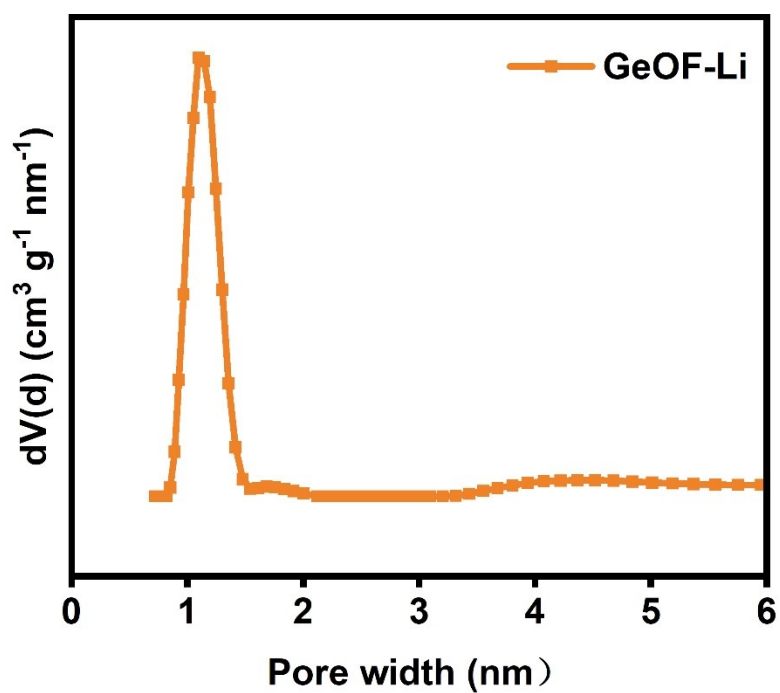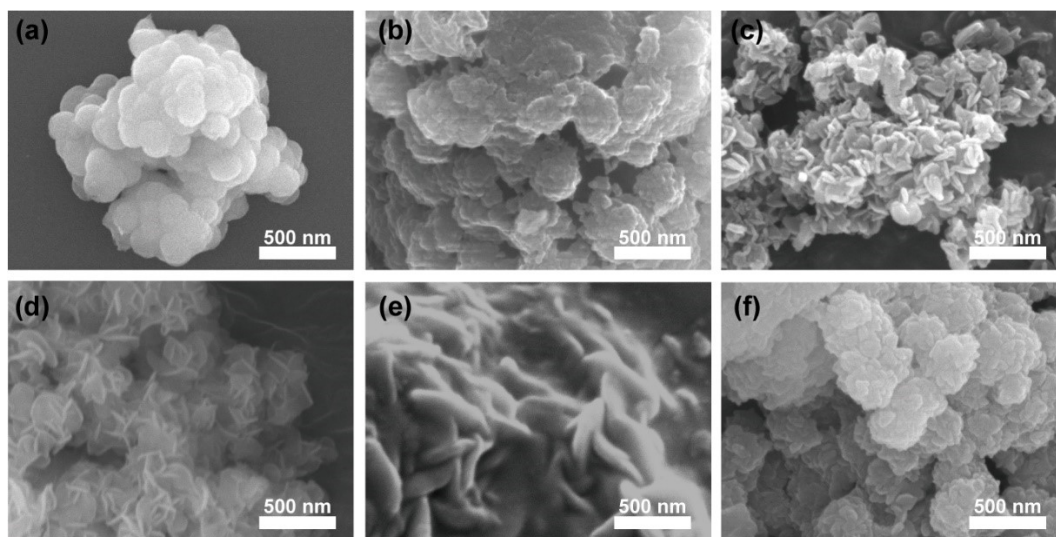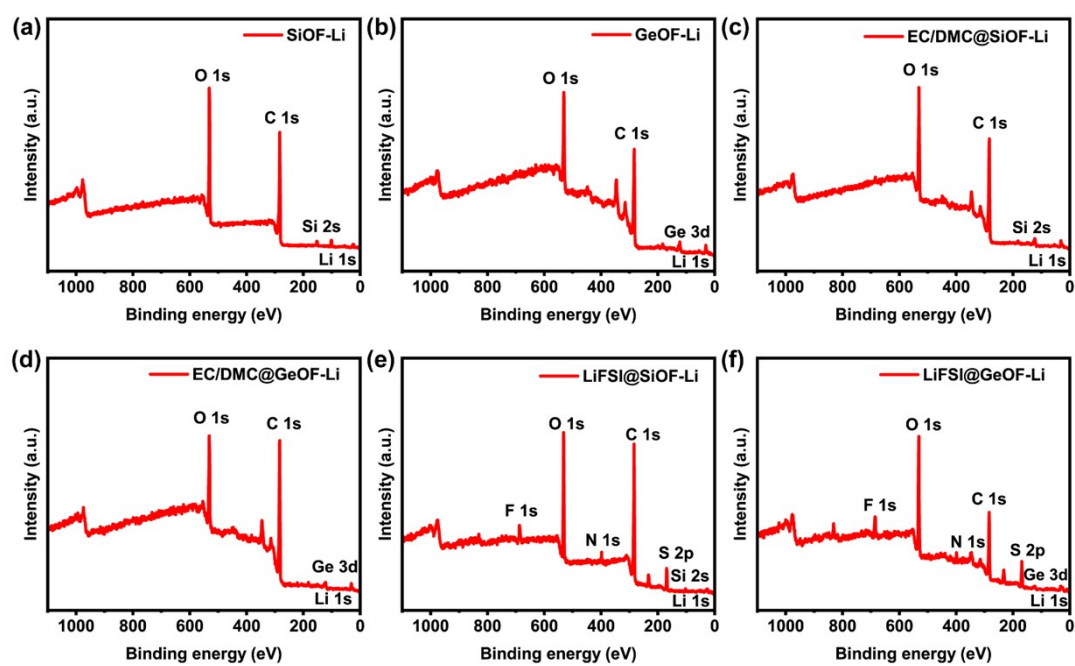**Fig. S3** Pore size distribution of SiOF-Li.

Fig. S4 Pore size distribution of GeOF-Li.

Fig. S5 SEM images of (a) SiOF-Li, (b) GeOF-Li, (c) EC/DMC@SiOF-Li, (d) EC/DMC@GeOF-Li, (e) LiFSI@SiOF-Li, and (f) LiFSI@GeOF-Li.

Fig. S6 XPS spectra of (a) SiOF-Li, (b) GeOF-Li, (c) EC/DMC@SiOF-Li, (d) EC/DMC@GeOF-Li, (e) LiFSI@SiOF-Li, (f) LiFSI@GeOF-Li.
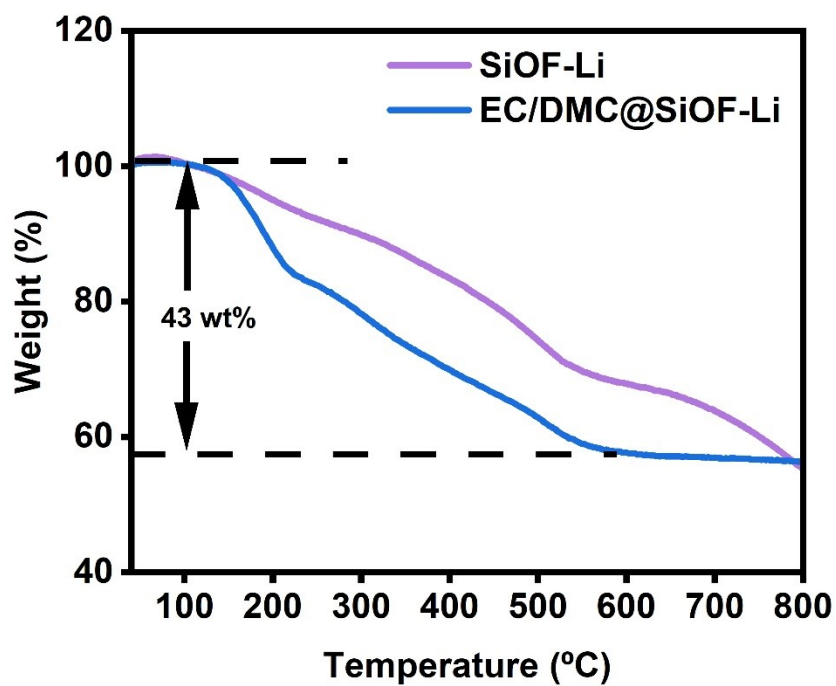
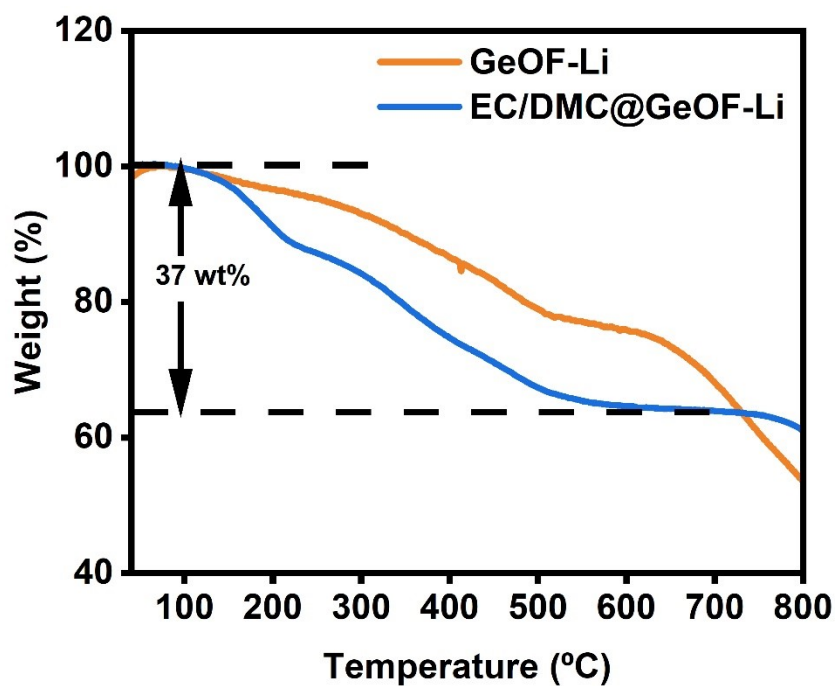**Fig. S7** TGA comparison of SiOF-Li and EC/DMC@SiOF-Li.

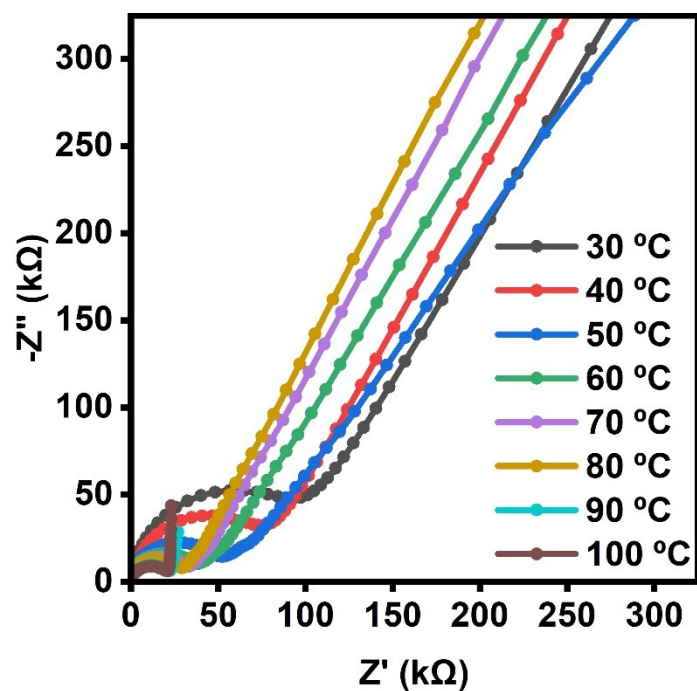**Fig. S8** TGA comparison of GeOF-Li and EC/DMC@GeOF-Li.

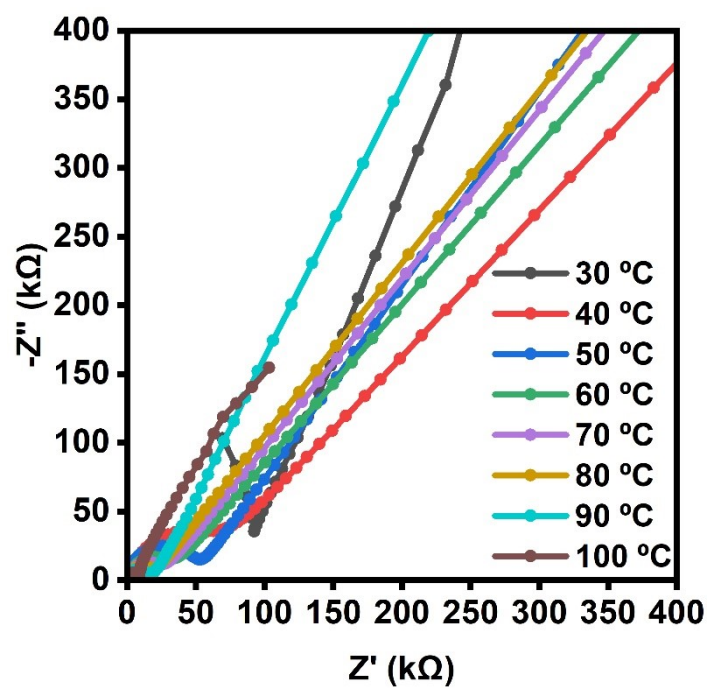**Fig. S9** Electrochemical impedance spectroscopies of pristine SiOF-Li at different temperatures.

Fig. S10 Electrochemical impedance spectroscopies of pristine GeOF-Li at different temperatures.
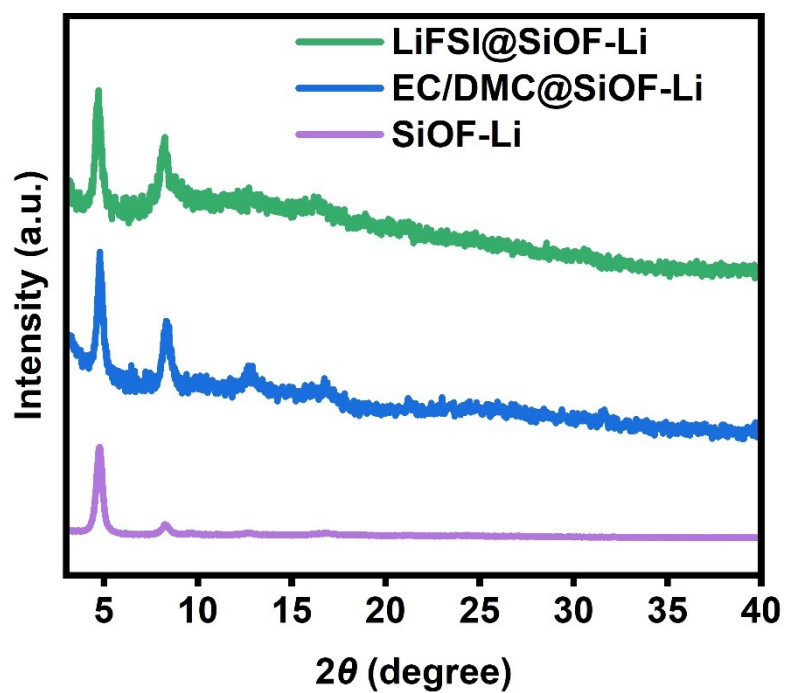
Fig. S11 PXRD patterns of SiOF-Li after immersing in EC/DMC and LiFSI solution.
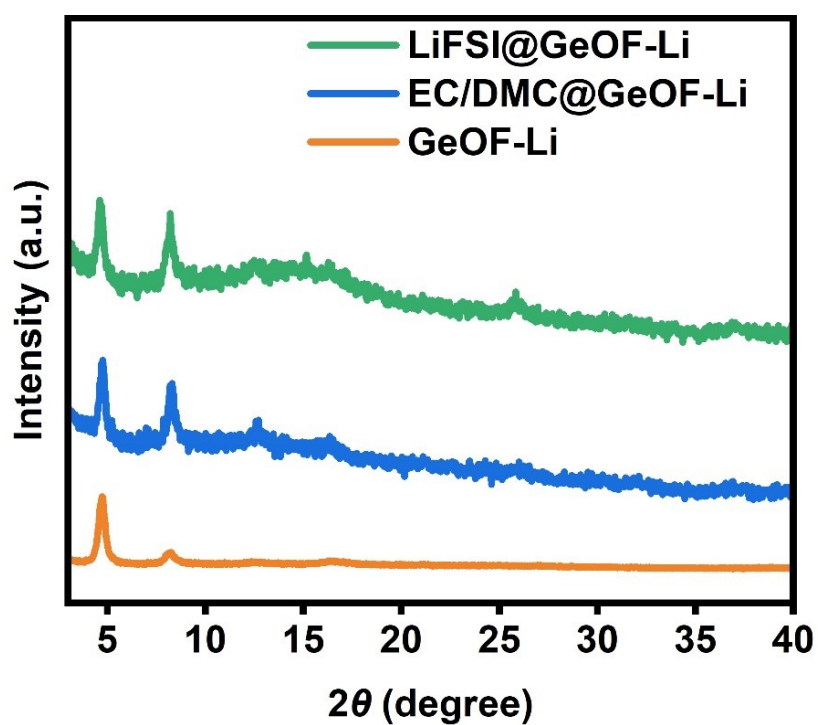

Fig. S12 PXRD patterns of GeOF-Li after immersing in EC/DMC and LiFSI solution.
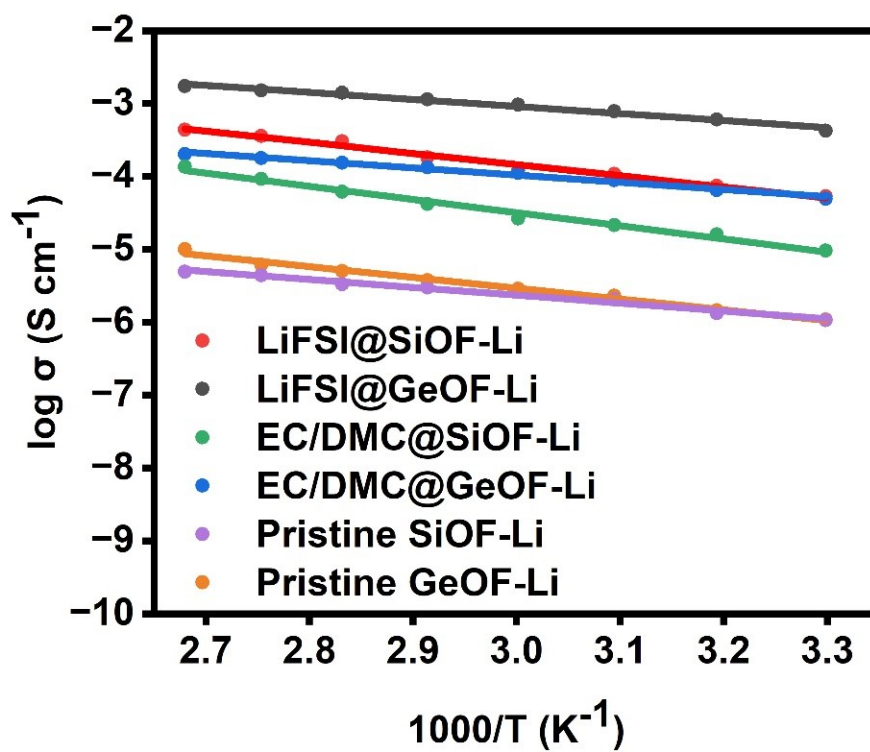
Fig. S13 Arrhenius plots of SiOF-Li and GeOF-Li at different conditions.

Fig. S14 TGA comparison of SiOF-Li and LiFSI@SiOF-Li.
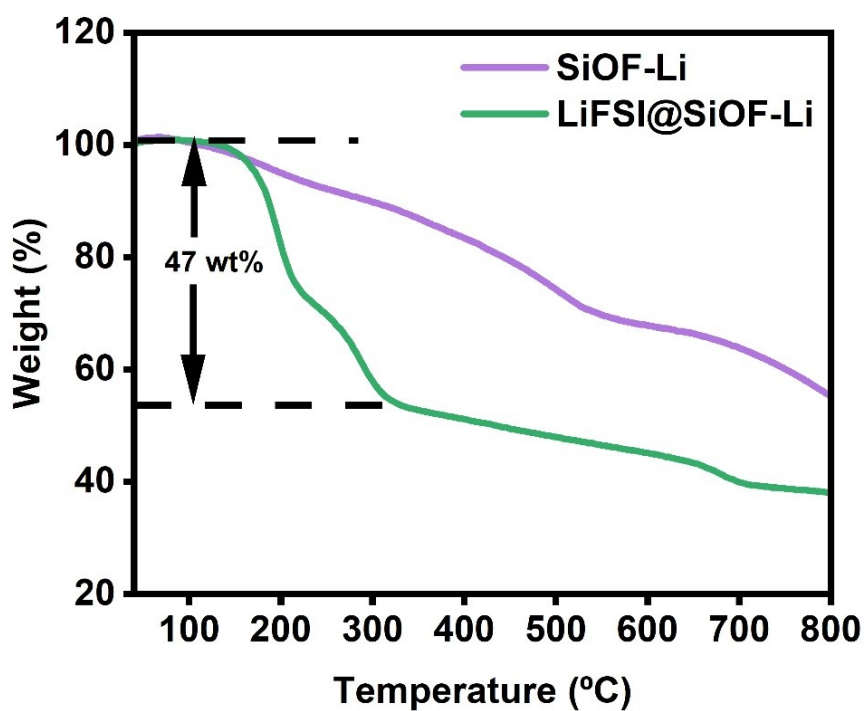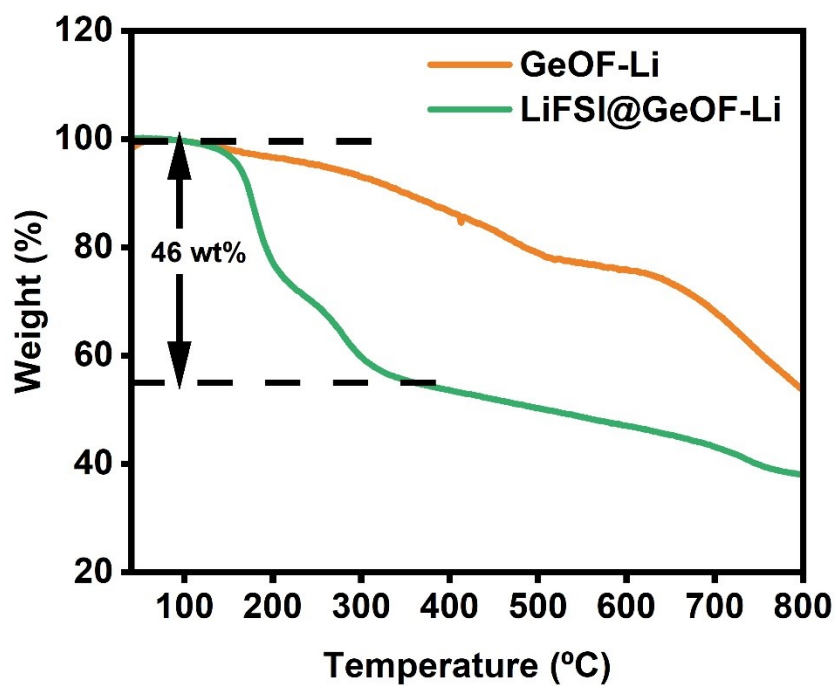
Fig. S15 TGA comparison of GeOF-Li and LiFSI@GeOF-Li.

Fig. S16 Electrochemical impedance spectroscopies of LiClO$_4$@SiOF-Li at different temperatures.
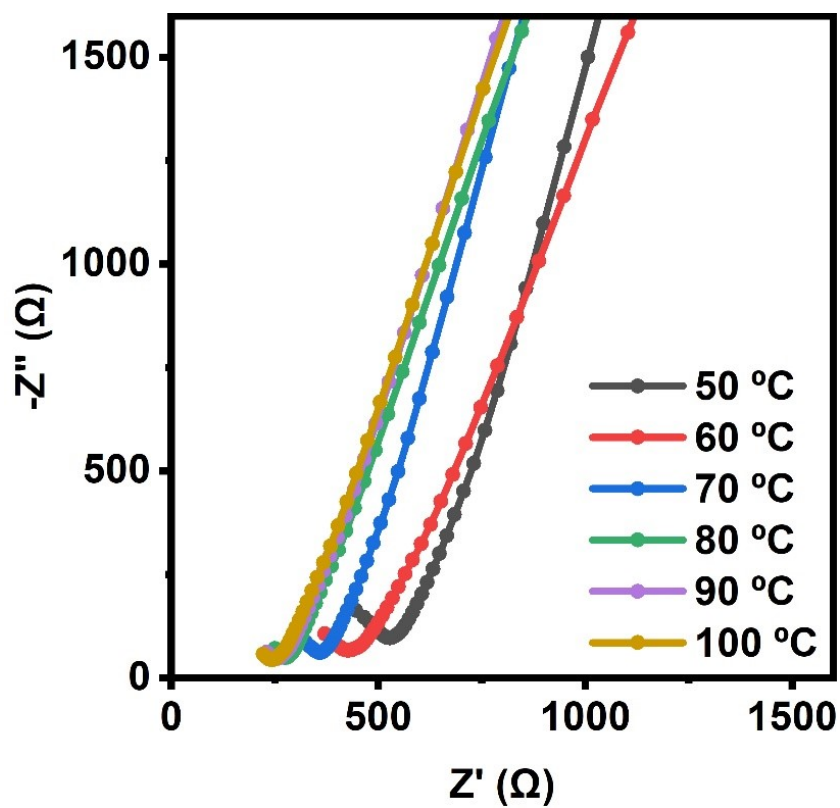
Fig. S17 Electrochemical impedance spectroscopies of LiClO$_4$@GeOF-Li at different temperatures.
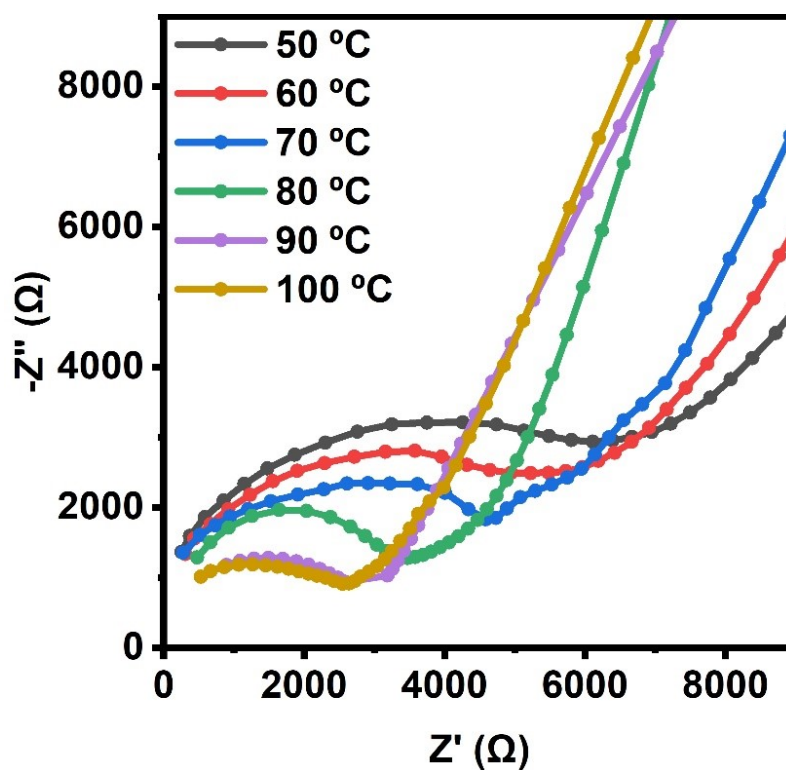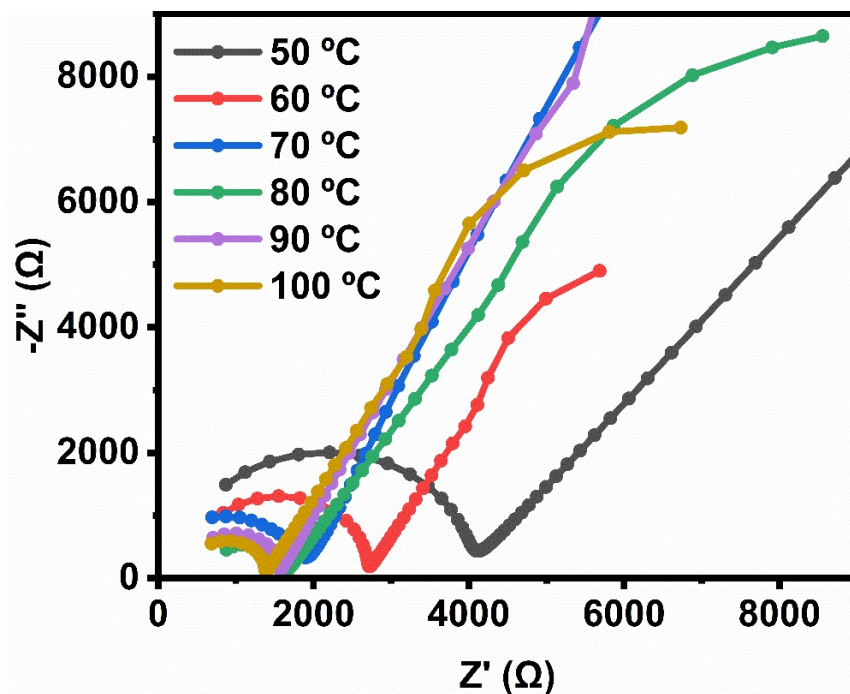

Fig. S18 Electrochemical impedance spectroscopies of LiTFSI@SiOF-Li at different temperatures.
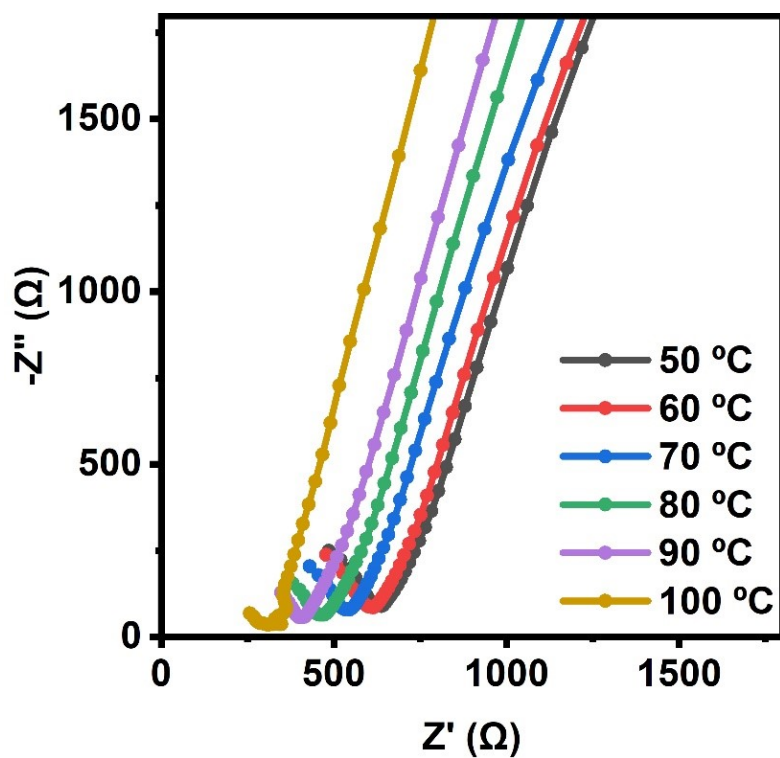
Fig. S19 Electrochemical impedance spectroscopies of LiTFSI@GeOF-Li at different temperatures.
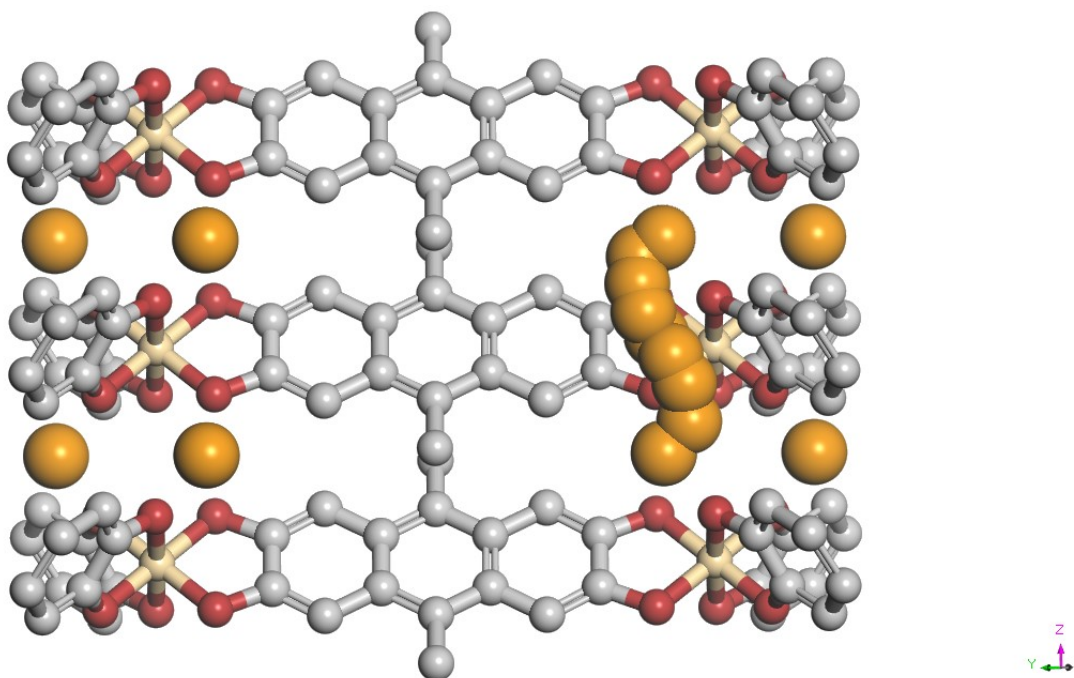
Fig. S20 The ion transport path of SiOF-Li. Note: C, grey; O, red; Si, beige; Li, orange, H are omitted for clarity.
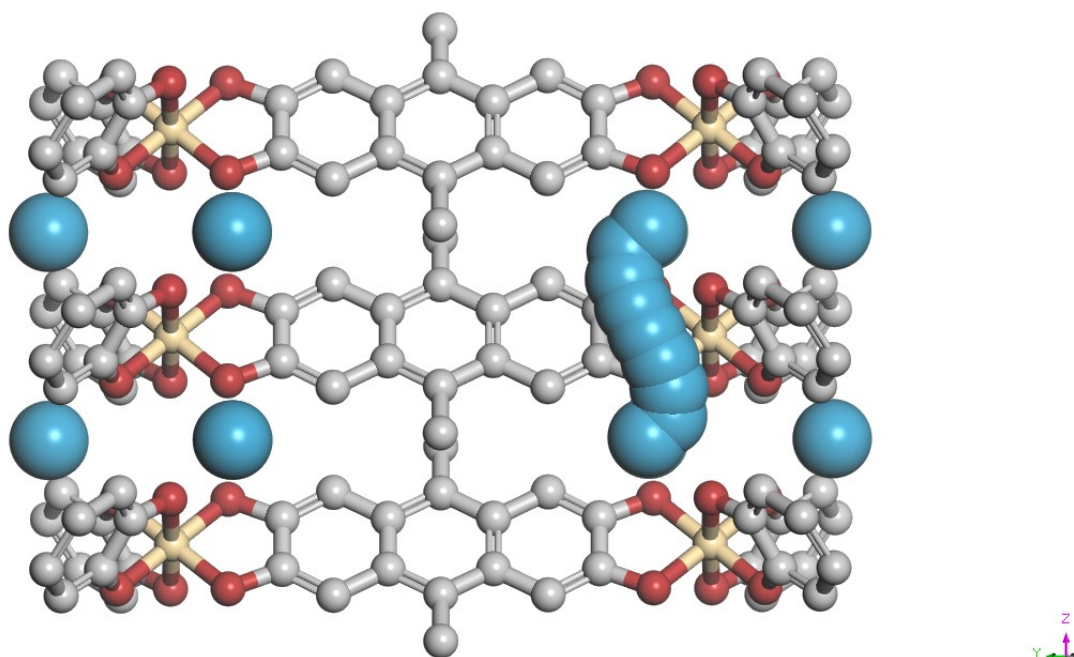
Fig. S21 The ion transport path of SiOF-Na. Note: C, grey; O, red; Si, beige; Na, blue, H are omitted for clarity.
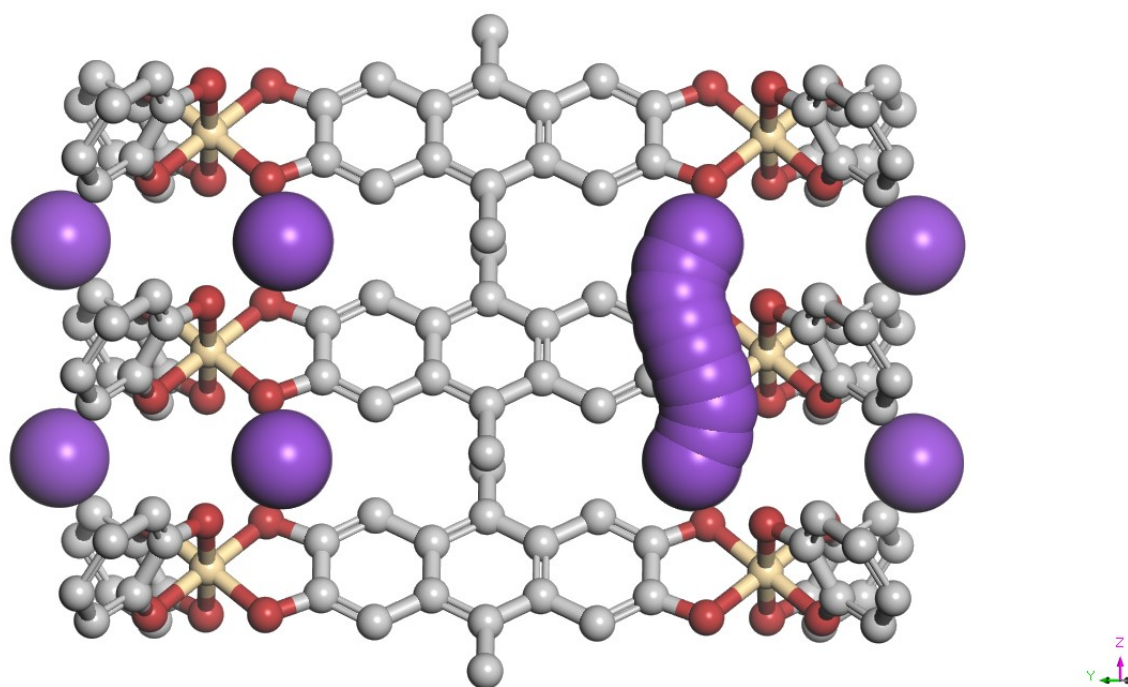
Fig. S22 The ion transport path of SiOF-K. Note: C, grey; O, red; Si, beige; K, purple, H are omitted for clarity.
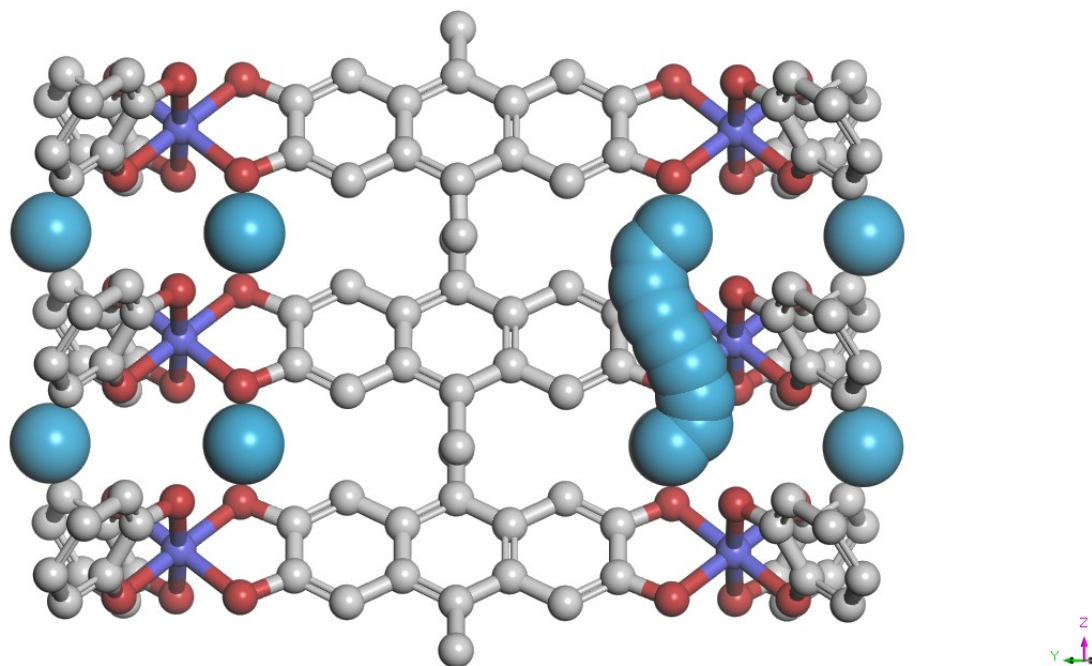
Fig. S23 The ion transport path of GeOF-Na. Note: C, grey; O, red; Ge, dark blue; Na, blue, H are omitted for clarity.
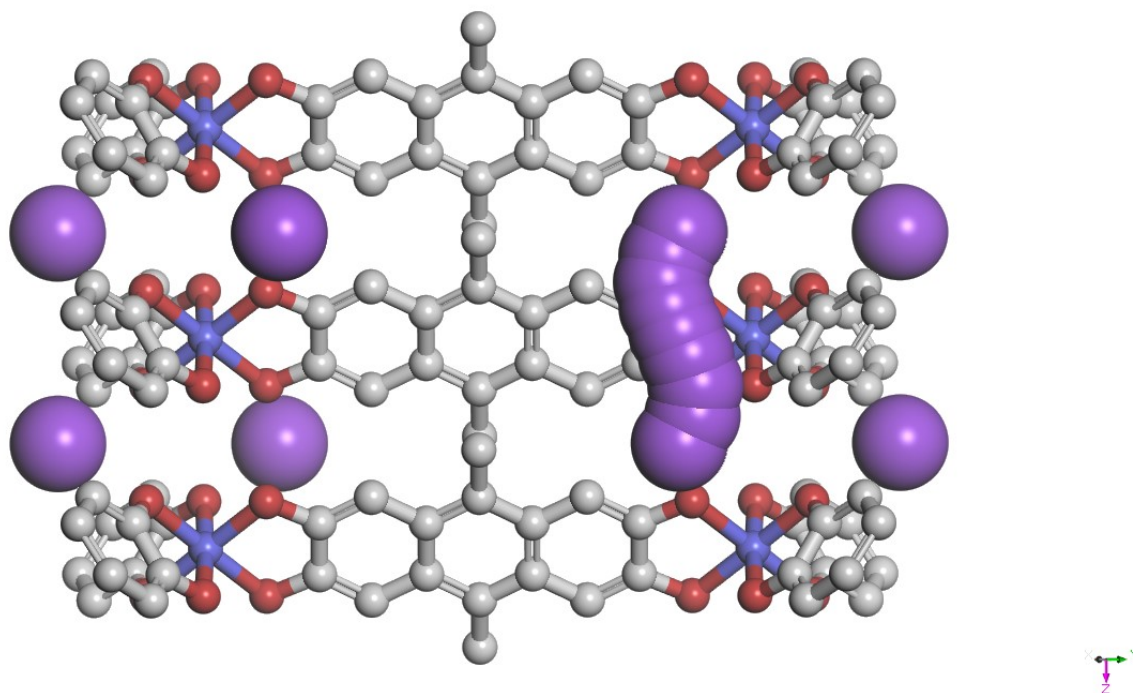
Fig. S24 The ion transport path of GeOF-K. Note: C, grey; O, red; Ge, dark blue; K, purple, H are omitted for clarity.

Table S1. Fractional atomic coordinates of the structural model of SiOF-Li.

SiOF-Li			
Hexagonal, *P31m* $a = b = 21.25000$ Å, $c = 4.62500$ Å $\alpha = \beta = 90.0000°$, $\gamma = 120.0000°$			
Atom	x/a	y/b	z/c
O	0.329010	0.595280	-0.210900
C	0.376780	0.574760	-0.108460

C	0.385930	0.519660	-0.209510
H	0.353370	0.487820	-0.351950
C	0.443180	0.508140	-0.107940
H	0.428560	0.391080	-0.584270
Li	0.461430	0.730710	0.500000
Si	0.333333	0.666667	0.000000
C	0.451840	0.451840	-0.215460
C	0.401540	0.401540	-0.445970
H	0.360770	0.360770	-0.357550

Table S2. Fractional atomic coordinates of the structural model of GeOF-Li.

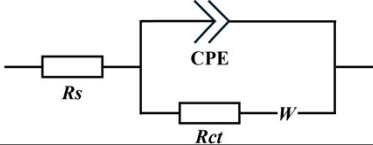| GeOF-Li			
Hexagonal, Hexagonal, *P31m*			
$a = b = 21.38670$ Å, $c = 4.81600$Å			
$\alpha = \beta = 90.0000^\circ$, $\gamma = 120.0000^\circ$			
Atom	x/a	y/b	z/c
O	0.32968	0.59474	-0.21379
C	0.37990	0.57821	-0.10737
C	0.38819	0.52219	-0.20997
H	0.34990	0.48924	-0.36634
C	0.44365	0.51007	-0.10753
H	0.43230	0.38662	-0.59222
Li	0.52903	0.76452	0.50000
Ge	0.33333	0.66667	0.00000
C	0.45397	0.45397	-0.21695
C	0.40476	0.40476	-0.44706
H	0.35725	0.35725	-0.35447

Table S3. The equivalent circuit and the fitted resistances of the electrochemical impedance spectroscopies.

Equivalent circuit			
Samples	R_s (Ω)	R_{ct} (Ω)	**Temperature (°C)**
SiOF-Li	57.1	94954	30
GeOF-Li	130.4	92655	30
EC/DMC@SiOF-Li	171.7	10979	30
EC/DMC@GeOF-Li	24.3	2032	30
LiFSI@SiOF-Li	109	1974	30
LiFSI@GeOF-Li	43.9	279.7	30

LiClO$_4$@SiOF-Li	77.9	6222	50
LiClO$_4$@GeOF-Li	54.6	604.9	50
LiTFSI@SiOF-Li	103.4	3603	50
LiTFSI@GeOF-Li	49.0	674.3	50

Table S4. Comparison of the lithium-ion conductivity of MetOFs with other MOFs.

Materials	Conductivity (S/cm)	Temperature (°C)	Ref.
SiOF-Li	1.0×10^{-6} 4.91×10^{-6}	30 100	*This work*
GeOF-Li	1.1×10^{-6} 1.0×10^{-5}	30 100	*This work*
EC/DMC@SiOF-Li	9.6×10^{-6} 1.36×10^{-4}	30 100	*This work*
EC/DMC@GeOF-Li	4.93×10^{-5} 2.68×10^{-4}	30 100	*This work*
LiFSI@SiOF-Li	5.32×10^{-5} 4.38×10^{-4}	30 100	*This work*
LiFSI@GeOF-Li	4.23×10^{-4} 1.72×10^{-3}	30 100	*This work*
LiClO$_4$@SiOF-Li	1.67×10^{-5} 4.0×10^{-5}	50 100	*This work*
LiClO$_4$@GeOF-Li	1.89×10^{-4} 4.1×10^{-4}	50 100	*This work*
LiTFSI@SiOF-Li	2.86×10^{-5} 8.3×10^{-5}	50 100	*This work*
LiTFSI@GeOF-Li	1.56×10^{-4} 3.0×10^{-4}	50 100	*This work*
MIT-20-LiCl	1.3×10^{-5}	25	4
MNFs@PEO	4.1×10^{-4}	60	5
P-PETEA-MOF	6.52×10^{-4}	r.t.	6
MOF-688(one-fold)	1.7×10^{-3}	r.t.	7
MOFs-NH$_2$	6.5×10^{-5}	r.t.	8
IL@MOF	1.03×10^{-3}	r.t.	9
Li@NKU-1000	1.13×10^{-3}	25	10

MIL-101(Cr)-DETA-Li	7.13×10^{-4}	30	11
CPE-0.5	6.22×10^{-3}	25	12

3. References

1. G. Kresse, D. Joubert, *Phys. Rev. B*, 1999, **59**, 1758.

2. G. Kresse, J. Furthmüller, *Comput. Mater. Sci.*, 1996, **6**, 15.

3. J.P. Perdew, K. Burke, M. Ernzerhof, *hys. Rev. Lett.*, 1996, **77**, 3865.

4. S. S. Park, Y. Tulchinsky and M. Dincă, *J. Am. Chem. Soc.*, 2017, **139**, 13260.

5. L. Wang, L. Xie, L. Dong, Z. Wang, L. Li, E. Shangguan, J. Li and S. Gao, *J. Colloid Interface Sci.*, 2024, **657**, 63.

6. J. Zhou, X. Wang, J. Fu, L. Chen, X. Wei, R. Jia and L. Shi, *Small*, 2024, **20**, 2309317.

7. T. Hou, W. Xu, X. Pei, L. Jiang, O. M. Yaghi and K. A. Persson, *J. Am. Chem. Soc.*, 2022, **144**, 13446.

8. L. Xu, X. Xiao, H. Tu, F. Zhu, J. Wang, H. Liu, W. Huang, W. Deng, H. Hou, T. Liu, X. Ji, K. Amine and G. Zou, *Adv. Mater.*, 2023, **35**, 2303193.

9. D.-H. Guan, X.-X. Wang, C.-L. Miao, J.-X. Li, J.-Y. Li, X.-Y. Yuan, X.-Y. Ma and J.-J. Xu, *ACS Nano*, 2024, **18**, 34299.

10. Z. Han, R. Zhang, J. Jiang, Z. Chen, Y. Ni, W. Xie, J. Xu, Z. Zhou, J. Chen, P. Cheng and W. Shi, *J. Am. Chem. Soc.*, 2023, **145**, 10149

11. G. Jiang, C. Qu, F. Xu, E. Zhang, Q. lu, X. Cai, S. Hausdorf, H. Wang and S. Kaskel, *Adv. Funct. Mater.*, 2021, **31**, 2104300.

12. J. Cao, X. Zhang, Y. Wang, S. Sha, Q. Wu, X. Sun and H.-G. Wang, *Chem. Eng. J.*, 2024, **502**, 157873.

13. Y. Xu, L. Gao, Q. Liu, Q. Liu, Z. Chen, W. Zhao, X. Kong and H. B. Wu, *Energy Storage Mater.*, 2023, **54**, 854.

14. S. Li, Y. Chen, X. Leng, M. Yang, W. U. Arifeen and T. J. Ko, *Chem. Eng. J.*, 2024, **500**, 157209.

15. Z. Guo, C. Guan, F. Li, S. Liao, X. Hao, J. Mu, Z. Huang, S. Wang and D. Cai, *J. Colloid Interface Sci.*, 2024, **683**, 1100.

16. S. Guo, Y. Su, K. Yan, C. Zhao, Y. Lu, H. Wang, J. Dong, N. Li, Y. Liu, Y. Guan, F. Wu and L. Chen, *Adv. Sci.*, 2024, **11**, 2404307.

17. Q. Li, Y. Yan, Z. Jiang, T. Chen and Q. Li, *Inorg. Chem.*, 2024, **63**, 10585.